



**Sudan University of Science and  
Technology**



**College of Graduate Studies**

## **Studying the I-V characteristics of Tunneling Resonant Diode**

**دراسة خصائص الجهد والتيار لثنائي الرنين النفقي**

**A Thesis Submitted in Partial Fulfillment of the Requirements for Degree  
of M. Sc. in Solid State Physics**

**Prepared By**

**Malaz Mohamed Osman Hassan**

**Supervisor**

**Dr. Isam Ahmed Attia**

**2021**

يقول الله تعالى

(شَهِدَ اللَّهُ أَنَّهُ لَا إِلَهَ إِلَّا هُوَ وَالْمَلَائِكَةُ  
وَأُولُو الْعِلْمِ قَائِمًا بِالْقِسْطِ ۗ لَا إِلَهَ إِلَّا  
هُوَ الْعَزِيزُ الْحَكِيمُ)

صدق الله العظيم

## *Dedication*

To myself .....

## **Acknowledgements**

Firstly, I would like to express my sincere gratitude to my Supervisor **Dr. Isam Ahmed Attia** for the continuous support of my Master degree study and related research, for his patience, motivation, and immense knowledge. His guidance helped me in all the time of research.

Secondly, I would like to express my sincere gratitude to my friend and brother **Ismail Mohamed Ismail** to provide a laptop computer for the purpose of implementing the research.

Third, I would like to express my sincere gratitude to my dear uncle **Sharaf Eldin Babiker** for my constant support.

## **Abstract**

A common problem in the tunneling diodes circuits is the I-V characteristic equation, the research concerns on a numerical simulation. This study describes the I-V characteristic equation Based on practical Resonant Tunneling Diode, it has adopted the I-V characteristic equation and transition to analyze the I-V equation using MATLAB. Special when these devices are biased in their negative differential resistance (NDR) region. The measured current-voltage (I-V) characteristics in the NDR region and current with voltage and a plateau like waveform in this region. Experimental equation validates to the Esaki model, and this is confirmed by the measured I-V characteristics.

## المستخلص

تعتبر معادلة الخصائص I-V مشكلة شائعة في دوائر الثنائيات النفقية، تتعلق هذه الدراسة بالحاكاة العددية.

و تصف هذه الدراسة المعادلة المميزة لخصائص الجهد والتيار للصلام الثنائي النفق الرنان العملي ، فقد تم ضبط معادلة الخصائص والانتقال باستخدام برنامج MATLAB لتحليل معادلة المنحنى المميز خاصة عندما تكون هذه الثنائيات متحيزة في منطقة المقاومة التفاضلية السلبية (NDR) . تم قياس خصائص الجهد والتيار (I-V) في منطقة NDR وشكل هضبة الموجة في هذه المنطقة وتم التحقق من صحة المعادلة التجريبية لنموذج Esaki، وهذا ما تؤكد خصائص I-V المقاسة والمحاكاة.

## Table of Contents

Topic	Page
Inductive page (الآية)	I
Acknowledgement	II
Dedication	III
Abstract (English)	IV
Abstract (Arabic)	V
Table of Content	VI
List of Symbols	IX
List of Figure	X
List of Table	XI

### Chapter One

#### Introduction

1.1	Background	1
1.2	Statement of the problem	2
1.3	Aims	3
1.4	Methodology	3
1.5	Questions	3
1.6	From literatures	4
1.7	Thesis lay out	5

### Chapter Two

#### Physics of Resonance Tunneling Diode

2.1	Introduction	7
2.2	Quantum Well	8
2.3	Resonant tunneling diodes	8
2.3.1	Principle of operation	10
2.3.2	Current – voltage characteristics	13
2.4	Review of tunnel diode and RTD theory	14
2.4.1	Esaki tunnel diode model	14
2.4.2	Esaki tunnel diodes	17

**Chapter Three**  
**Empirical Equation for I-V Characteristic of the Resonant Tunneling Diode**

<b>3.1</b>	Introduction	<b>21</b>
<b>3.2</b>	Direct characterization of I-V characteristics	21
<b>3.3</b>	Result	21
<b>3.4</b>	Discussion	22

**Chapter Four**

**Conclusion & Future Work**

<b>4.1</b>	Introduction	25
<b>4.2</b>	Conclusion	25
<b>4.3</b>	Future Work	25
	Reference	27

### List of Symbols /Abbreviations

c	Capacitance
$\epsilon_0$	is the permittivity of free space
$\epsilon_r$	is the relative permittivity of the barrier and well materials
A	is the area of the device
d	is the width of the double barriers quantum well structure
t	is the thickness of the double barrier quantum well structure that consists of the layer of the spacer
PVCR	peak to valley current ratio
IP	peak current density
IV	valley current density
$V_{bi}$	is the built-in potential voltage,
$V_j$	the voltage across the p-n junction
$V_t$	is the thermal voltage
q	is the elementary charge
r	is the relative permittivity of the material
CMOS	Complementary metal-oxide semiconductor
TD	Tunneling diode
$V_p$	Peak voltage
$V_v$	Valley voltage
$n^*$	Effective carrier concentration

## List of Figures

Figure no.	Figure Title	Page
<b>1.1</b>	Current-voltage characteristic of a commercial silicon tunnel diode	
<b>2.1</b>	A cross-section of a resonant tunneling diode and the corresponding conduction band diagram under forward bias, and the corresponding I-V curve. $E_{cE}$ and $E_{fE}$ are the conduction band and Fermi-level of the emitter, respectively, and $E_{cC}$ and $E_{fC}$ are the conduction band and Fermi-level of the collector, respectively, and $V_{bias}$ is the forward bias voltage. a) The cross-section of a resonant tunneling diode, b) conduction band diagram without forward bias $V_{bias} = 0$ , c) conduction band diagram with forward bias at peak voltage $V_{bias} = V_p$ , d) conduction band diagram with forward bias at valley voltage $V_{bias} = V_v$ . e) Typical current-voltage characteristic of a tunnel diode [46], [52].	
<b>2.2</b>	Esaki tunnel diode model	
<b>2.3</b>	Evaluation of total current and voltage as a function of the state variable.	
<b>2.4</b>	Cross-section of a tunnel diode and the corresponding band diagram. $E_{cp}$ , $E_{vp}$ and $E_{fp}$ are the conduction band, valence band and Fermi-level of the p-type semiconductor, respectively, and $E_{cn}$ , $E_{vn}$ and $E_{fn}$ are the conduction band, valence band and Fermi-level of the n-type semiconductor, respectively, and $V_{bias}$ is the forward bias voltage. a) The cross-section of a tunnel diode, b) band diagram without forward bias $V_{bias} = 0$ , c) band diagram with forward bias at peak voltage $V_{bias} = V_p$ , d) band diagram with forward bias at valley voltage $V_{bias} = V_v$ . [46], [48].	
<b>2.5</b>	Typical current-voltage characteristic of a tunnel diode [46].	
<b>2.6</b>	A typical RTD IV-curve. At a certain applied voltage, the current reaches a maximum; further increase of the voltage causes a decrease of current. This is the negative differential region. Increasing the voltage even further causes the current to increase rapidly due to thermionic emission.	

<b>3.1</b>	A circuit for direct I-V measurement of tunnel diodes or general NDR devices. An external capacitor $C_e$ is introduced in series with $R_e$ .	
<b>3.2</b>	Measured I-V characteristics for a) tunnel diode 1N3717 and b) tunnel diode 1N3714 without bias and high frequency stabilization. The curves in the NDR region have the characteristic ‘plateau’ distortion due to bias oscillations	
<b>3.3</b>	Measured current-voltage (I-V) characteristics for tunnel diode 1N3714	
<b>3.4</b>	First (a) and second (b) derivatives of the I-V curve of the ‘stabilized’ 1N3717 tunnel diode (Fig. 3.7(a)). Here $R_e = 8$ . The valley/peak in the second derivative shows the presence of oscillations in the 90 mV to 180 mV range of the NDR region.	
<b>4.1</b>	Final drawing of the empirical equation by MATLAB	

## List of tables

<b>Table no.</b>	<b>Title</b>	<b>Page</b>
<b>2.1</b>	parameter	
<b>4.1</b>	Experiment points	

# Chapter One

## Introduction

### 1.1 Background

The development and progress of microelectronics have made it possible to facilitate daily life by creating new technologies in all fields. This development is accompanied by a miniaturization of various components. This reduction in the characteristic dimensions leads to a degradation of the components (increase in the leakage current, etc.) and the loss of certain application functions. Among the solutions proposed, we note the replacement of the classical switches by diodes but also the use of semiconductor components to provide other new functionalities.

Indeed, the discovery of interesting characteristics, for example, Zener diode has a unique characteristic which is operating in forward and reverse bias thus produces the stable reference voltage. Hence, it is widely used in power supplies. Resonant Tunneling Diode (RTD) which is also a powerful device that will be discussed in this study on its unique current-voltage characteristics.

The resonant tunnel diode, also known as the Esaki diode, was first discovered by Leo Esaki in 1957[1] when exploring internal field emission in heavily doped reverse biased germanium p-n junctions. The operation of tunnel diode depends on the quantum mechanics principle known as “Tunneling”. In electronics, tunneling means a direct flow of electrons across the small depletion region from n-side conduction band into the p-side valence band. He observed the distinctive N shaped current-voltage (I-V) characteristic of this same junction when biased in the forward bias direction similar to the I-V characteristic of the Si tunnel diode shown in Fig 1.1:

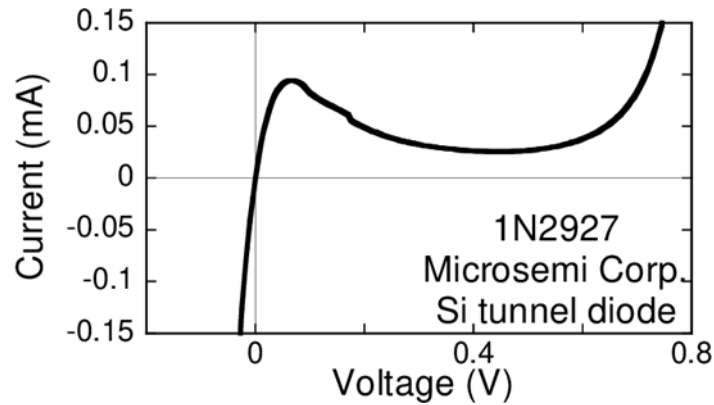


Figure 1.1: Current-voltage characteristic of a commercial silicon tunnel diode [2]

A semiconductor has a forbidden region where there are no states available for its electrons. This region called the band gap. The states below this gap (which comprise the valence band) are almost all filled. The states above it (the conduction band) are almost empty. The number of empty states in valence band, or electrons in the conduction band, can be controlled by adding either acceptor impurities or donor impurities to the semiconductor crystal. Each acceptor impurity takes one electron out of the valence band, and each donor gives one electron to the conduction band. In this way p-type (empty states in valence band) and n-type (electrons in conduction band) regions can be built into a crystal. The nonlinear I-V characteristic of an Esaki tunnel diode originates from electron transport across a degenerately doped p+n+ junction

## 1.2 Statement of the problem

In 1973, Tsu and Esaki discovered the tunneling effect in superlattices. In the next year, Chang et al. reported the resonant tunneling effect in double barrier semiconductor structures [2]. More than 30 years have passed and RTDs have now been widely developed and utilized in microelectronics and optoelectronics. All these applications are largely based on two unique properties of the RTD: the negative differential resistance (NDR) and the bistability in the NDR region. Fig. 1.4 shows schematically the operation principle of the RTD. When the bias is gradually increased, the difference between the Fermi level in the emitter and the

quasi sublevel in the QW between the two barriers approach each other. When the two levels are aligned, the penetration of the electron wave function through the barriers becomes very long and resonant tunneling occurs.

research concerns on a numerical simulation, to describe the evolution the Based on practical Resonant Tunneling Diode, we have adopted the I-V characteristic equation and transition to analyze the I-V equation using MATLAB.

### **1.3 Aims**

The objectives of this project are as follows:

1. To Find the physic-based equation of the resonant tunneling diode to determine the current-voltage characteristics of the device in MATLAB
2. To fit the current-voltage characteristic of the resonant tunneling diode of physic-based model to experimental data by empirical fitting
3. To develop a circuit model and simulated I-V characteristics of resonant tunneling diode

### **1.4 Methodology**

Many physical phenomena can be modelled by differential equations, but -apart from some very specific cases – it is generally not possible to write down the solution to these problems in closed form. In order to understand the behavior of the solution, it is thus often necessary to construct an approximation via a numerical solution.

Our research concerns on an empirical equation, to describe the evolution the

- Find the equation of the empirical curve
- Determine the highest point at the peak and the lowest point at the valley

### **1.5 Questions**

- \* What is I-V characteristic for tunneling effect diode equation?
- \* From the empirical equation how many peaks are possible in the curve?
- \* Do the experimental equations differ with the doping density?

## 2.5 From literatures

In order to verify the reliability of the developed solver we simulated I-V characteristics of various kinds of RTDs from literatures [8, 10, and 11]. One of the structures we simulated is the relatively simple structure from Mattia et. al. [11]. The diodes they studied had simple quantum well, thick barriers and long spacer in the collector side. Figure 2.9 compares the measured I-V curve by Mattia et. al. with our calculation.

The diode studied by Auer et. al. [8] consists of composite InGaAs/InAs materials for QW with short spacers and relatively thin symmetric barriers. Our simulation is compared with their measured static characteristics in figure 2.6.

Figure 2.9: The experimental I-V characteristic from Mattia et. al. [11-13] and our self-consistent simulation. The nominal thickness of the barrier and QW are 4.1 nm and 5.5 nm respectively. But their simulation resulted in a peak current density 2.3 times higher than measurement although the peak voltage was matching well. So in order to match the I-V curves they increase the barrier thickness to 4.5 nm for their simulations.

The barrier thickness used in our simulation is 4.0 nm with the QW width of 5.5 nm.

Our simulation considers same doping densities in the emitter and collector regions as the reported nominal values. In their diode they have  $2 \times 10^{16} \text{ cm}^{-3}$  doping concentration in the spacers and  $2 \times 10^{18} \text{ cm}^{-3}$  dopants in the emitter and collector. They were using 10 nm spacer in the emitter side and 100 nm spacer in the collector side. Inset shows the conduction band diagram for the studied RTD.

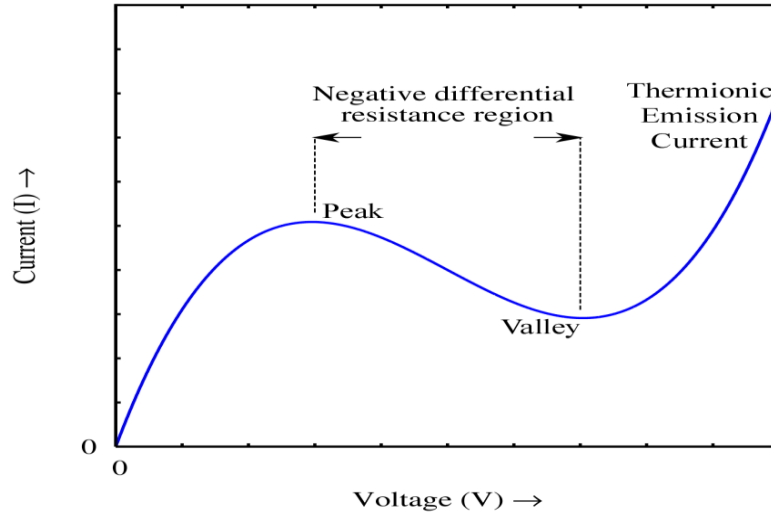


Figure 1.2: A typical RTD IV-curve. At a certain applied voltage, the current reaches a maximum, further increase of the voltage causes a decrease of current. This is the negative differential region. Increasing the voltage even further causes the current to increase rapidly due to thermionic emission.

### 1.6 Thesis lay out

This thesis is organized into four chapters. Chapter 1 would discuss the project background of resonant tunneling diode, problem statements, project objectives and also project scopes, Chapter 2 is the literature review of the thesis. The previous work on resonant tunneling diode will be discussed in this chapter. It stated the problem statement and methodology on the previous journals that have been studied as references to complete this study, Chapter 3 is about the methodology of the thesis. This chapter describes how to model and simulate RTD model and analyze I-V characteristics. Empirical fitting will be discussed in this chapter for comparing models and measured data. Besides that, developing a circuit model of RTD in LT Spice IV will also be explained in this chapter, Chapter 4 is about the result and discussion. This chapter contains the results of modelling and simulation of RTD using MATLAB and its current-voltage characteristics. The empirical fitting result for both model and measured data will be discussed in this chapter. Besides that, an RTD circuit model which was developed and simulated in LT Spice IV will also be discussed in this chapter

concludes all the results that have been gathered. Some suggestions for the future improvement will be stated in this chapter.

## Chapter Two

### Physics of Resonance Tunneling Diode

#### 2.1 Introduction

A resonant-tunneling diode (RTD) is a diode with a resonant-tunneling structure in which electrons can tunnel through some resonant states at certain energy levels. The current–voltage characteristic often exhibits negative differential resistance regions.

All types of tunneling diodes make use of quantum mechanical tunneling. Characteristic to the current–voltage relationship of a tunneling diode is the presence of one or more negative differential resistance regions, which enables many unique applications. Tunneling diodes can be very compact and are also capable of ultra-high-speed operation because the quantum tunneling effect through the very thin layers is a very fast process. One area of active research is directed toward building oscillators and switching devices that can operate at terahertz frequencies.

An RTD can be fabricated using many different types of materials (such as III–V, type IV, II–VI semiconductor) and different types of resonant tunneling structures, such as the heavily doped p–n junction in Esaki diodes, double barrier, triple barrier, quantum well, or quantum wire. The structure and fabrication process of Si/SiGe resonant interband tunneling diodes are suitable for integration with modern Si complementary metal–oxide–semiconductor (CMOS) and Si/SiGe heterojunction bipolar technology.

One type of RTDs is formed as a single quantum well structure surrounded by very thin layer barriers. This structure is called a double barrier structure. Carriers such as electrons and holes can only have discrete energy values inside the quantum well. When a voltage is placed across an RTD, a terahertz wave is emitted, which is why the energy value inside the quantum well is equal to that of

the emitter side. As voltage is increased, the terahertz wave dies out because the energy value in the quantum well is outside the emitter side energy.

Another feature seen in RTD structures is the negative resistance on application of bias as can be seen in the image generated from Nanohub. The forming of negative resistance will be examined in detail in operation section below.

This structure can be grown by molecular beam heteroepitaxy. GaAs and AlAs in particular are used to form this structure. AlAs/InGaAs or InAlAs/InGaAs can be used.

The operation of electronic circuits containing RTDs can be described by a Linard system of equations, which are a generalization of the Van der Pol oscillator equation

## **2.2 Quantum Well**

Quantum wells play an enormous role in microelectronics and are found in many different shapes and forms [2].

RTD has undergone the process of quantum tunneling phenomena via double barrier quantum well. Quantum well is formed when a narrow of band gap semiconductor is sandwiched in between two wider band gap layers. The wider band gap layer is known as the barrier while a narrow band gap is known as a well in double barrier quantum well structure.

## **2.3 Resonant tunneling diodes**

A resonant tunneling diode (RTD) consists of three parts: 1) an emitter region, which is the source of electrons, 2) a double-barrier quantum-well (DBQW) structure which consists of a low band-gap quantum-well material sandwiched between two barriers of high band-gap material, 3) a collector region to collect the electrons tunneling through the double-barrier structure. The emitter and collector regions are made of heavily doped n-type semiconductors. The cross section and the corresponding conduction band diagram of an RTD are given in Fig. 2.1. The double-barrier structure is designed such that resonant energy levels are present in the quantum-well. Electrons from the emitter can tunnel through the

barriers if their longitudinal energy is equal to one of the resonant energy levels in the quantum-well.

As shown in the band diagram of Fig. 2.1, if the forward bias (positive on the collector) is zero, there is no current because the electrons from the emitter cannot quantum mechanically tunnel through the double-barriers structure (Fig. 2.1(b)). When the forward applied bias is small, electrons from the emitter form an accumulation layer near the barrier and a small fraction of electrons reach the first resonant energy level and then can tunnel through the double-barriers structure, leading to a small current. As the voltage increases, the first resonant energy level (E1) of the quantum-well is moved downwards to the Fermi level of the emitter (EFE). A great number of electrons from the emitter can tunnel through the double-barriers structure into the collector, which leads to an increasing current with the forward bias. This continues until the maximum current  $I_p$  is reached when the first resonant energy level reaches (E1) the bottom of the conduction band of emitter (EcE) which means that the overlap between the region of incident electrons from the emitter and the first resonant level region reaches a maximum (Fig. 2.1(c)). When a larger voltage is applied, fewer electrons from the emitter can go across the double barriers and the diode current rapidly drops and a negative differential resistance (NDR) region is produced. For even larger applied voltages, thermal emission over the barrier and tunneling through the non-resonant energy levels of the well become important and the diode current rises rapidly (Figure 2.1(d)).

Since the double barrier structure is an undoped region sandwiched between two heavily doped regions, the device capacitance can be given approximately by

$$C_n = \frac{A\varepsilon_0\varepsilon_r}{d} \quad (2.1)$$

where,  $\varepsilon_0$  is the permittivity of free space,  $\varepsilon_r$  is the relative permittivity of the barrier and well materials, A is the area of the device and d is the width of the double barriers quantum well structure, i.e. consists of the width of the barrier

layers, the quantum well and any spacer layers [3]. Unlike the tunnel diode junction capacitance which varies with bias, the RTD capacitance is largely bias independent.

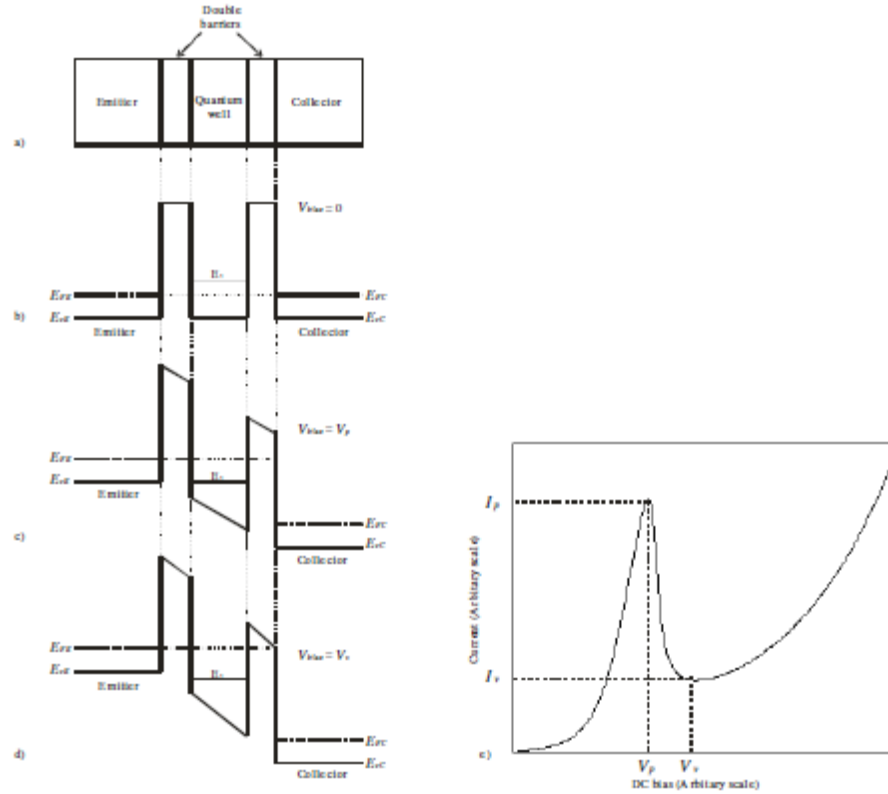


Figure 2.1: A cross-section of a resonant tunneling diode and the corresponding conduction band diagram under forward bias, and the corresponding I-V curve.  $E_{cE}$  and  $E_{fE}$  are the conduction band and Fermi-level of the emitter, respectively, and  $E_{cC}$  and  $E_{fC}$  are the conduction band and Fermi-level of the collector, respectively, and  $V_{bias}$  is the forward bias voltage. a) The cross-section of a resonant tunneling diode, b) conduction band diagram without forward bias  $V_{bias} = 0$ , c) conduction band diagram with forward bias at peak voltage  $V_{bias} = V_p$ , d) conduction band diagram with forward bias at valley voltage  $V_{bias} = V_v$ . e) Typical current-voltage characteristic of a tunnel diode [4], [5].

### 2.3.1 Principle of Operation

Tunneling diodes provide the same functionality as a CMOS transistor where under a specific external bias voltage range, the device will conduct a current thereby switching the device “on”. However, instead of the current going through

a channel between the drain and source as in CMOS transistors, the current goes through the depletion region by tunneling in normal tunneling diodes and through quasi-bound states within a double barrier structure in RTDs. A TD consists of a p-n junction in which both the n- and p-regions are degenerately doped ( $>10^{19} \text{ cm}^{-3}$ ). There is a high concentration of electrons in the conduction band (EC) of the n-type material and empty states in the valence band (EV) of the p-type material. Initially, the Fermi level ( $E_F$ ) is constant because the diode is in thermal equilibrium with no external bias voltage. When the forward bias voltage starts to increase, the  $E_F$  will start to decrease in the p-type material and increase in the n-type material. Since the depletion region is very narrow ( $<10 \text{ nm}$ ), electrons can easily tunnel through, creating a forward current as shown in Figure 1. Depending on how many electrons in the n-region are energetically aligned to the empty states in the valence band of the p-region, the current will either increase or decrease. As the bias voltage continues to increase, the ideal diffusion current will cause the current to increase. When a reverse-bias voltage is applied, the electrons in the p-region are energetically aligned with empty states in the n-region causing a large reverse-bias tunneling current.

The current-voltage (I-V) curve shows the negative differential resistance (NDR) characteristic of RTDs. For a specific voltage range, the current is a decreasing function of voltage. This property is very important in the circuit implementation because it can provide for the different voltage-controlled logic states corresponding to the peak and valley currents. RTDs utilize a quantum well with identically doped contacts to provide similar I-V characteristics. It consists of two heavily doped, narrow energy-gap materials encompassing an emitter region, a quantum well in between two barriers of large band gap material, and a collector region, as shown in Figure 3. A current method of growth for this device is Metal Organic Chemical Vapor Deposition using GaAs-AlGaAs. The quantum-well thickness is typically around 5nm and the barrier layers are around 1.5 to 5 nm thick. When there is no forward voltage bias, most of the electrons and holes are

stationary forming an accumulation layer in the emitter and collector region respectively. As a forward voltage bias is applied, an electric field is created that causes electrons to move from the emitter to the collector by tunneling through the scattering states within the quantum well. These quasi-bound energy states are the energy states that allow for electrons to tunnel through creating a current. As more and more electrons in the emitter have the same energy as the quasi-bound state, more electrons are able to tunnel through the well, resulting in an increase in the current as the applied voltage is increased. When the electric field increases to the point where the energy level of the electrons in the emitter coincides with the energy level of the quasi-bound state of the well, the current reaches a maximum, as shown in Figure 2.2. Resonant tunneling occurs at specific resonant energy levels corresponding to the doping levels and width of the quantum well. As the applied voltage continues to increase, more and more electrons are gaining too much energy to tunnel through the well and the current is decreased. After a certain applied voltage, current begins to rise again because of substantial thermionic emission where the electrons can tunnel through the non-resonant energy levels of the well. This process produces a minimum “valley” current that can be classified as the leakage current.

RTDs have a major advantage over TDs. When a high reverse bias voltage is applied to TDs, there is a very high leakage current. However, RTDs have the same doping type and concentration on the collector and emitter side. This produces a symmetrical I-V response when a forward as well as a reverse bias voltage is applied. In this manner the very high leakage current present in normal TDs is eliminated. Thus, RTDs are very good rectifiers. RTD bandwidths were reported for InAs/AlSb RTDs at about 1.24 THz due to their low ohmic contact resistance and short transit times. Higher bandwidths could be obtained using InAs Schottky-contact RTDs (SRTDs) because of the higher tunneling current densities and shorter transit times. However, InGaAs/AlAs/InP is usually used instead of InAs/AlSb because of its mature fabrication and growth technologies.

### 2.3.2 Current -Voltage Characteristics

Resonant tunneling diode has negative differential resistance (NDR) in I-V characteristics due to the effects of tunneling in semiconductor. NDR occurs when there is a transverse momentum conversion condition in epitaxial growth crystal. NDR formed in I-V characteristics when there are no electrons in the emitter can pass through the quantum well during the conservation of transverse momentum. This will lead to sharp decreasing the current density from its maximum value. NDR influences the speed and the frequency of the device. Sharp NDR will lead to high-speed and high-frequency devices. High frequency is regarding to the small value of device capacitance, hence, have high frequency operation. Equation can find the approximation of device capacitance [1]

$$C_d = \frac{A\varepsilon_0\varepsilon_r}{t} \quad (2.2)$$

Where A is the area of the device. and are presenting the permittivity of free space and the relative permittivity of the barrier and well materials. t is the thickness of the double barrier quantum well structure that consists of the layer of the spacer, barrier and well. Resonant Tunneling Diode is a nanometer device which has nanometer thickness layers. This resulting very small capacitance, thus, has high-frequency devices.

Furthermore, the NDR properties were given advantages in digital circuit design. NDR properties will lead to reducing the complexity in the logic circuit. It has the ability to create a bistable or multi-stable circuit and switching between two stable states can be very fast. Meanwhile, in they have validated the NDR characteristics of InGaN/InAlN/GaN/InAlN RTD. They have found that greater NDR can be obtained when uses the In composition in  $\text{In}_x\text{Ga}_{1-x}\text{N}$  is around 0.06. Furthermore, a sharp negative differential resistance will offer a low power consumption of the resonant tunneling diode. Consequently, it will reduce the static and dynamic power dissipation during switching or without switching operations.

In addition, peak to valley current ratio (PVCR) is an important parameter since the performance of the resonant tunneling diode depends on the peak to valley current ratio. High peak current density will have efficient performance of RTD. High PVCR indicates the device has high-speed transient response. High-speed transient response is very useful in high-speed switching applications. Apparently, the equation denoted that  $I_P$  must be large in order to get high PVCR. Nevertheless, too large peak current will have a large power dissipation.  $I_P$  and  $I_V$  are presenting the peak current density and valley current density, respectively.

$$PVCR = \frac{I_P}{I_V} \quad (2.2)$$

## **2.4 Review of tunnel diode and RTD theory**

### **2.4.1 Esaki tunnel diode model**

The intrinsic Esaki tunnel diode model consists of an ideal tunnel diode a nonlinear capacitor and a nonlinear resistor, see Fig 2.2. There are two controlling variables in this model, which are an as yet unspecified time-dependent state variable, and its time derivative. The ideal tunnel diode is modelled using current and voltage as a function of the primary state variable  $x$ . The capacitance is modelled by using the evaluated voltage and the time derivative of the state variable,  $dx/dt$ , to calculate the derivative of charge as a function of time or  $dq/dt$ . From this, the current through the capacitor can be determined. The resistor is modelled using the evaluated voltage and the total current. An outline of the model calculation of the total current and voltage is shown in Fig 2.3.

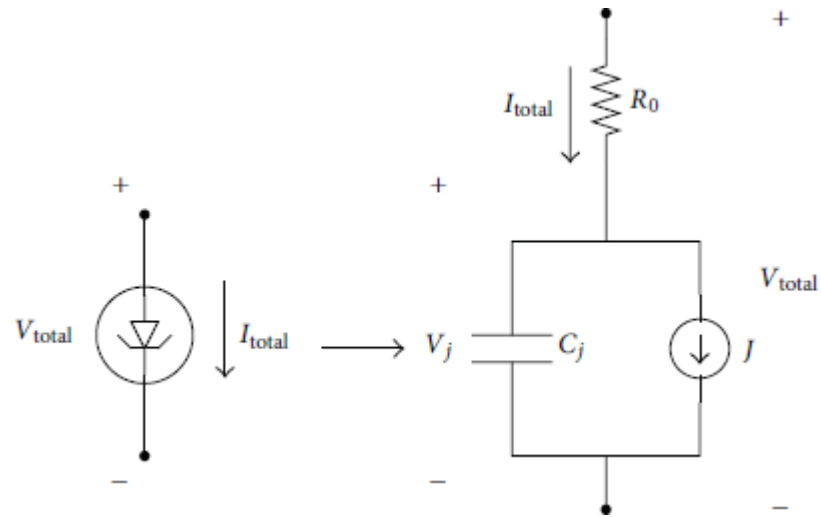


Figure 2.2: Esaki tunnel diode model

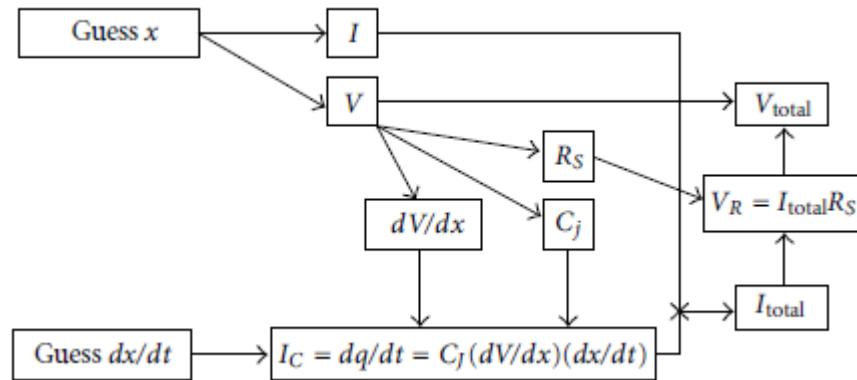


Figure 2.3: Evaluation of total current and voltage as a function of the state variable.

The tunnel diode current density is typically described as the sum of three exponential functions derived from quantum mechanical considerations. This formulation appears in Sze [4], although here the physics is limited only to the forward-bias direction. Referring to Figure 2.3.

The first term is a closed-form expression of the tunneling current density which describes the behavior particular to the tunnel diode. This includes the negative resistance region which captures the core functionality of the tunnel diode. The second term describes the excess tunneling current density while the third term is the normal diode characteristic. In [5],  $J_P$  is the peak current density and  $V_P$  is the corresponding peak voltage. In [6],  $J_V$  is the peak current density and  $V_V$  is the corresponding peak voltage.

The parameter  $A_2$  represents an excess current perfector.

Finally, in [7],  $J_S$  is the saturation current density,  $q$  is the charge of an electron,  $k$  is Boltzmann's constant, and  $T$  is the temperature in degrees Kelvin.

As mentioned in the previous section, the exponential functions can lead to a rapid change in current for a relatively small change in voltage which can create convergence issues for the simulator's nonlinear solver.

The tunnel diode equation cannot be solved for current as a single and unique function of voltage. Recognizing that the three major components of current density can be thought of as three diodes with exponential I-V characteristics, they are parameterized as previously described. After individual parameterization of the three regions based on equating current density and first derivatives at threshold points, the tunnel diode equations become

$$\begin{aligned}
 v(t) &= \begin{cases} V_0 + \frac{1}{\alpha} \ln\{1 + \alpha[x(t) - V_0]\}, & V_0 \leq x(t), \\ x(t), & x(t) \leq V_0, \end{cases} \\
 i(t) &= \begin{cases} I_s \exp(\alpha V_0) \{1 + \alpha[x(t) - V_0]\} - I_s, & V_0 \leq x(t), \\ I_s [\exp(\alpha v(t)) - 1], & x(t) \leq V_0, \end{cases} \quad (3.2)
 \end{aligned}$$

where (3) is the exact parametric representations of the diode I-V characteristic. The highly nonlinear I-V characteristic is now transformed into current-state-variable (I-X) and voltage-state-variable (V-X) characteristics that are not as strongly nonlinear, without any changes to the essential mathematical model of the device. The solution is well behaved and local convergence or heuristics within the diode model are not required. After the transformations of (3), the reduced nonlinear nature of the relationship is illustrated in Figure 2, the I-X relationship, and in Figure 3, the V-X relationship, with  $I_s = 100$  aA,  $\alpha = 38.686$ , and  $V_0 = 0.8$ V.

Table 2.1: parameter

Parameter	Description	Default	Units
JS	Saturation current	$1 \times 10^{-16}$	A
CTO	Zero bias depletion capacitance	0	F
FI	Built-in barrier potential	0.8	V
GAMA	Capacitance power law parameter	0.5	—
CDO	Zero bias diffusion capacitance	0	F
AFAC	Slope factor of diffusion capacitance	38.696	1/V
RO	Series resistance in forward bias	0	$\Omega$
TAU	Intrinsic depletion layer time constant	0	sec
AREA	Area multiplier	1	—
JV	Valley current	$1 \times 10^{-4}$	A
JP	Peak current	$1 \times 10^{-3}$	A
VV	Valley voltage	0.5	V
VPK	Peak voltage	0.1	V
A2	Excess current prefactor	30	—
MT	Tunnel current slope factor	-1	—
MX	Excess current slope factor	1	—
MTH	Thermal current slope factor	1	—
TEMP	Temperature	300°	K

### 2.4.2 Esaki Tunnel diodes

Tsu and Esaki [6] first proposed the resonant tunneling structure. Heavily doped p-type and n-type semiconductors are used to build tunnel diodes. A p-type semiconductor is doped with acceptor impurities and an n-type semiconductor is doped with donor impurities. The Fermi-level (energy level where the probability of an available state being occupied by an electron is equal to 50 percent) of the intrinsic semiconductor is at the center of the band gap [4]. However, for the doped semiconductors, the Fermi-level moves towards the valence band edge with increasing acceptor concentration or moves towards to the conduction band edge with increasing donor concentration [4,6].

A cross section of a tunnel diode is shown in Fig. 1.2(a), which is a p-n junction structure made of heavily doped semiconductors (carrier concentrations of  $10^{19}$  per  $\text{cm}^3$  to  $10^{20}$  per  $\text{cm}^3$ ) [5, 7]. The n-type semiconductor contains so many donor impurities that all of the states near the bottom of the conduction band are occupied by electrons so that the Fermi-level moves up into the conduction band instead of being located in the band gap (right side of Fig. 2.4). On the other hand, the p-type semiconductor contains so many acceptor impurities that all of the states near the top of the valence band are emptied of electrons so that the Fermi-

level moves into the valence band instead of being located in the band gap (left side of Fig. 2.4).

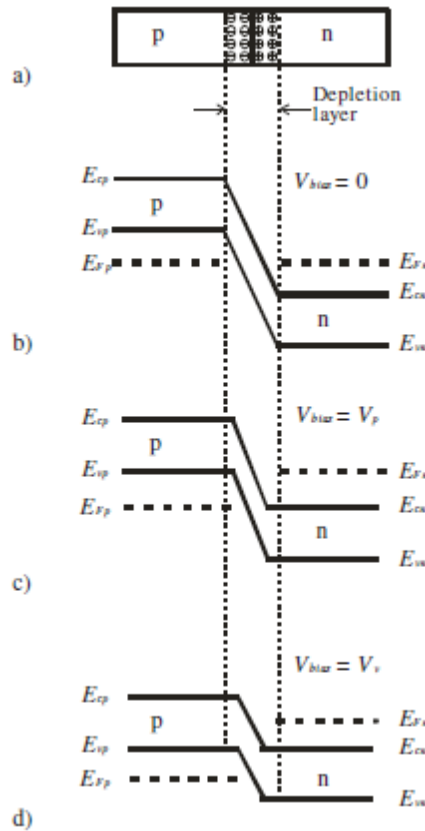


Figure 2.4: Cross-section of a tunnel diode and the corresponding band diagram.  $E_{cp}$ ,  $E_{vp}$  and  $E_{fp}$  are the conduction band, valence band and Fermi-level of the p-type semiconductor, respectively, and  $E_{cn}$ ,  $E_{vn}$  and  $E_{fn}$  are the conduction band, valence band and Fermi-level of the n-type semiconductor, respectively, and  $V_{bias}$  is the forward bias voltage. a) The cross-section of a tunnel diode, b) band diagram without forward bias  $V_{bias} = 0$ , c) band diagram with forward bias at peak voltage  $V_{bias} = V_p$ , d) band diagram with forward bias at valley voltage  $V_{bias} = V_v$ . [4], [6].

With no applied forward bias, no current flows through the junction (Fig. 1.2(b)). Then if a small forward (positive on the p-type semiconductor) bias is applied, it causes a large number of the electrons at the bottom of the conduction band of the n-type semiconductor to tunnel through to the top of the valence band of the p-type semiconductor. With increasing forward bias, a larger forward

current flows through the junction because the overlap between the region between the Fermi-level and valence band of p-type semiconductor ( $E_{Fp}$  and  $E_{vp}$ ) and the region between the Fermi-level and conduction band of n-type semiconductor ( $E_{Fn}$  and  $E_{cn}$ ) increase. When the forward bias reaches the peak voltage ( $V_p$ ) which means the overlap reaches maximum, the tunneling current reaches its peak current  $I_p$  (Fig. 2.4(c)). When the forward voltage is further increased, there are fewer available unoccupied states in the p-type semiconductor. Therefore, the current decreases with the increasing forward bias and negative differential resistance (NDR) region is produced. When the forward bias reaches the valley voltage ( $V_v$ ), the bands are almost “uncrossed” and there are almost no unoccupied states in the p-type semiconductor available for tunneling. Therefore, the tunneling current reaches its valley current  $I_v$  (Fig. 2.4(d)). With still further increase of the voltage the normal thermal current will flow [4], [6]. Fig. 2.5 shows a typical current-voltage (I-V) characteristic of tunnel diode with forward bias. The depletion layer introduces a junction depletion capacitance, which is bias dependent, and it is given by[7].

$$\frac{1}{C_n^2} = \frac{2(V_{bi} - V_j - 2V_T)}{A^2 q \epsilon_r n^*} \quad (2.4)$$

where  $C_n$  is the junction capacitance of tunnel diode,  $V_{bi}$  is the built-in potential voltage,  $V_j$  is the voltage across the p-n junction,  $V_T$  is the thermal voltage,  $A$  is junction area,  $q$  is the elementary charge and  $\epsilon_r$  is the relative permittivity of the material used to form the tunnel diode. The  $n^*$  is the effective carrier concentration [8,9].

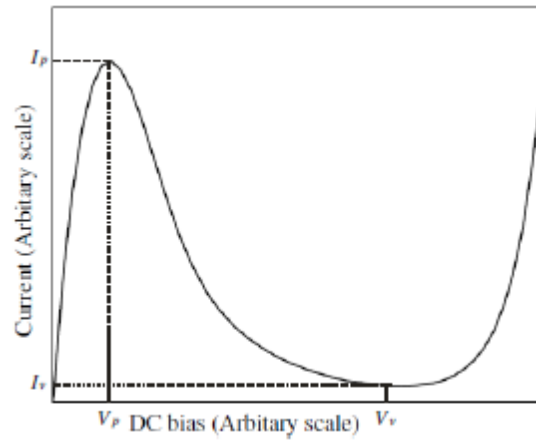


Figure 2.5: Typical current-voltage characteristic of a tunnel diode [4].

## Chapter Three

# Empirical Equation for I-V Characteristic of The Resonant Tunneling Diode

### 3.1 Introduction:

In this chapter, a technique is demonstrated for a physical empirical equation based I-V Characteristic of tunnel diode, to the Esaki tunnel diode model describing the operation of a device and requires no modification to the underlying algorithms of a circuit simulator. A similar approach can be used for other strongly nonlinear devices.

### 3.2 Direct characterization of I-V characteristics

Using the circuit of Fig. 2.5, the diodes I-V characteristics can be measured indirectly. If direct I-V characterization is desired, then a capacitor  $C_e$  can be introduced in the circuit as shown in Fig.3.1

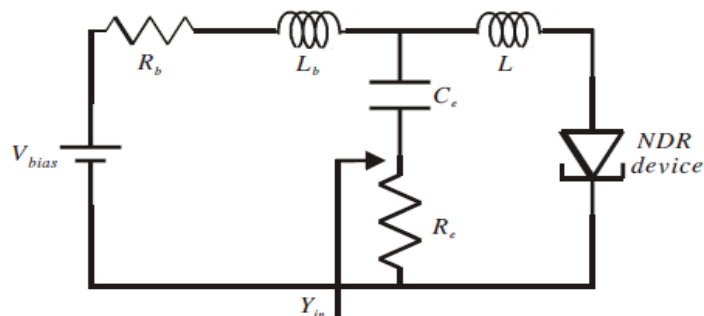


Figure 3.1: A circuit for direct I-V measurement of tunnel diodes or general NDR devices. An external capacitor  $C_e$  is introduced in series with  $R_e$ .

### 3.3 Results

Commercially available 1N3717 and 1N3714 tunnel diodes from American Micro semiconductors were used in the experimental work. The I-V characteristics of the tunnel diodes were measured by Agilent B1500 semiconductor device analyzer (SDA) in steps of 5 mV. Measured I-V characteristics without bias stabilization are shown in table.3.1. These measurements show the characteristic

"plateau" distortion due to bias oscillations, but I and V for the 1N3717 and 1N3714 tunnel diodes, respectively, could be noted.

Table 31: Experiment points

<b>V/mV</b>	<b>I/mA 1N3717</b>	<b>I/mA 1N3714</b>
0	0.0	0.0
10	0.5	0.1
20	2	0.3
30	2.7	0.5
40	4.0	0.7
50	4.5	1
60	4.3	1.5
70	3.2	1.7
80	3.1	2
90	3	2.25
100	2.8	2.3
150	2.5	1.5
200	2.0	1.2
250	1.0	0.7
300	0.5	0.6
350	0.6	0.5
400	0.8	0.3
450	1.0	0.8

### 3.4 Discussion

The equation derivative of measured I-V curves can be used to detect the presence of other peaks in the curves

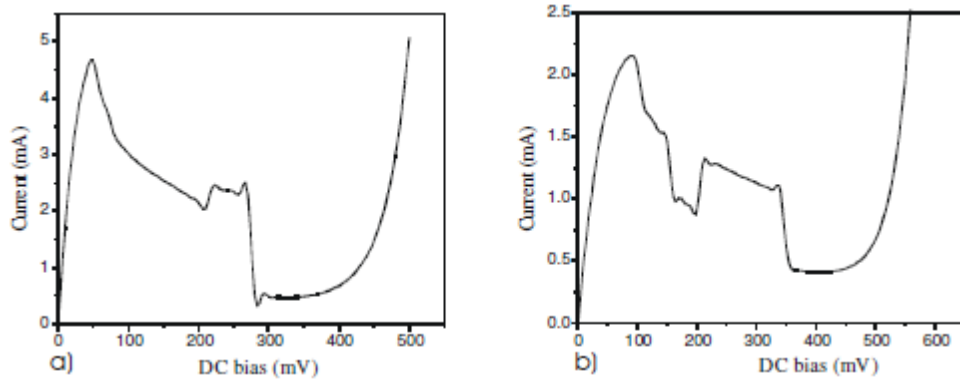


Figure 3.2: Measured I-V characteristics for a) tunnel diode 1N3717 and b) tunnel diode 1N3714 without bias and high frequency stabilization. The curves in the NDR region have the characteristic ‘plateau’ distortion due to bias oscillations.

As can be seen from Fig.3.2 for unsterilized devices, there is a fast decrease of current around the peak current area if the oscillations are present. This fast decrease of current results in a valley in the first derivative of I-V curve, and therefore, the second derivative curve will show a sharp valley immediately followed by a sharp peak. The second derivative will show the characteristics of same a sharp valley immediately followed by a sharp peak. This pair of the oscillation characteristics in the second derivative curve can be used to detect whether there are

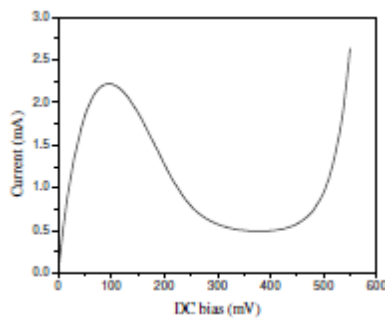


Figure 3.3: Measured current-voltage (I-V) characteristics for tunnel diode 1N3714

The criteria for designing test fixtures for the DC characterization of tunnel diodes was developed and experimentally verified. The developed approach can also be used to accurately measure the current-voltage characteristics of RTDs

on-wafer. Although the capacitance of a RTD (10 -100 fF range) which is much smaller than the capacitance of a tunnel diode (10 - 100 pF range), it is still

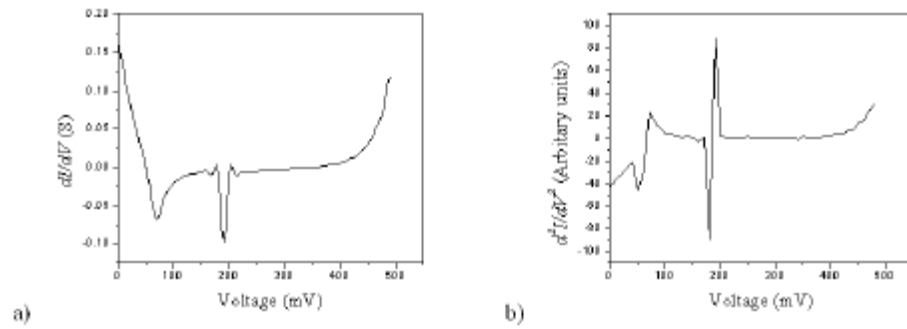


Figure 3.4: First (a) and second (b) derivatives of the I-V curve of the ‘stabilized’ 1N3717 tunnel diode (Fig. 3.7(a)). Here  $R_e = 8$  . The valley/peak in the second derivative shows the presence of oscillations in the 90 mV to 180 mV range of the NDR region.

## Chapter Four

### Conclusion

#### 4.1 Introduction:

The study generally presents the mechanism of

#### 4.2 conclusions

Tunneling is an important aspect of charge transport in semiconductor and molecular devices. While a semiconductor tunnel diode with characteristics described by sums of exponential functions was considered, the parameterization technique introduced can be used with any analytic expression.

The central result is transcribing a circuit simulation problem from one dealing with strong nonlinearities to one working with well-behaved, moderately nonlinear element characteristics. This is achieved without an increase in problem size. The introduction of an alternative state (or state variable) enables the strongly nonlinear character of tunneling to be modelled, with full accuracy, by intermediate equations which are relatively well behaved and moderately nonlinear. Thus, off-the-shelf numeric can be used in a circuit simulator and there is no need for local heuristics, homotopy, or functional approximation to obtain convergence. The fundamental requirement is that the circuit simulator support state variables. The state variables replace the (usual) nodal voltages as the unknowns and the error function becomes the energy norm rather than solely based on Kirchoff's Current Law while the total number of unknowns remains unchanged.

#### 4.3 Future Work

The results obtained show that I-v Curve of RTD is reliable. Further research is however required to investigate the reliability of the proposed techniques at millimeter-wave and submillimeter-wave frequencies.

The stabilized DC and RF characterization circuit techniques developed in the thesis for tunnel diodes will make it possible to develop accurate small and large signal models for RTDs. Such models will be invaluable to the future reliable design of RTD-based circuits.

## Reference

- [1] L. L. Chang, L. Tsu and T. Esaki, "Resonant tunneling in semiconductor double barriers," *Applied Physics Letters*, vol. 24, no. 12, pp. 593-595, June 1974.
- [2] S. M. Sze, "High-speed semiconductor devices," John Wiley & Sons, 1990.
- [3] I. Mehdi, G. I. Haddad, and R. K. Mains, "Device performance criteria for resonant tunneling diodes as microwave and millimeter-wave sources," *Microwave and Optical Technology Letters*, vol. 2, no. 5, pp. 172-175, May 1989.
- [4] J. M. Carrol, "Tunnel diode and semiconductor circuits," McGraw-Hill Book Company, Inc. 1963. 209
- [5] P. Roblin and H. Rohdin, "High-speed heterostructure devices: from device concepts to circuit modelling," Cambridge University Press, 2002.
- [6] R. N. Hall, "Tunnel diodes," *IRE Transactions on Electron Devices*, vol. 7, no. 1, pp. 1-9, 1960.
- [7] M. W. Dashiell, J. Kolodzey, P. Crozat, F. Aniel and J. M. Lourtioz, "Microwave properties of silicon junction tunnel diodes grown by molecular beam epitaxy," *IEEE Electron Device Letters*, vol. 23, no. 6, June 2002.
- [8] M. W. Dashiell, R. T. Troeger, T. N. Adam, P. R. Berger, J. Kolodzey, A. C. Seabaugh and R. Lake, "Current voltage characteristics of high current density silicon Esaki diodes grown by molecular beam epitaxy and the influence of thermal annealing," *IEEE Transactions on Electron Devices*, vol. 47, no. 9, pp. 1707-1714, Sep. 2000.
- [9] S. Sze, "Physics of semiconductor devices," 2nd edition, New York, Wiley, 1985.
- [10] V. Radisic, X. B. Mei, W. R. Deal, W. Yoshida, P. H. Liu, J. Uyeda, M. Barsky, L. Samoska, A. Fung, T. Gaier, R. Lai, "Demonstration of submillimeter wave fundamental oscillators using 35-nm InP HEMT technology," *IEEE Transactions on Microwave Theory and Techniques*, vol. 17, no. 3, pp. 223-225, Mar. 2007.
- [11] M. Asada, S. Suzuki and N. Kishimoto, "Resonant tunneling diodes for sub terahertz and terahertz oscillators," *Japanese Journal of Applied Physics*, vol. 47, no. 6, pp. 4375-4384, 2008.
- [12] O. Boric-Lubecke, D.-S. Pan and T. Itoh, "DC instability of the series connection of tunneling diodes," *IEEE Transactions on Microwave Theory and Techniques*, vol. 44, no. 6, pp. 936-943, June 1996.

[13] O. Boric-Lubecke, D.-S. Pan, and T. Itoh, "RF Excitation of an Oscillator with Several Tunneling Devices in series," *IEEE Microwave and Guided Wave Letters*, vol. 4, no. 11, pp. 364-366, Nov. 1994.